JASA EXPRESS LETTERS ARTICLE asa.scitation.org/journal/jel

Reduction of inertial end correction of perforated plates due to secondary high amplitude stimuli

Ralf Burgmayer, Friedrich Bake, and Lars Enghardt[a)]
German Aerospace Center, Berlin, 10623, Germany
ralf.burgmayer@dlr.de, friedrich.bake@dlr.de, lars.enghardt@dlr.de

Abstract: The decrease in reactance of perforated plates at high sound pressure amplitudes is of interest for the design of Helmholtz resonator liners. It is associated with the loss of end correction due to flow separation at the orifices. In practical applications, complex acoustic signals impinge on perforations. The loss of end correction due to multiple stimuli of unrelated frequency and phase has not been considered yet. This study assesses and presents an empirical approximation for the reduction of end correction of perforated plates at primary frequencies when flow separation is induced by an additional secondary unrelated high amplitude stimulus.

[Editor: Mark Sheplak] https://doi.org/10.1121/10.0009920

Received: 15 October 2021 **Accepted:** 9 March 2022 **Published Online:** 1 April 2022

1. Introduction

With rising sound pressure, the impedance of orifices and perforated plates becomes dependent on the particle velocity inside the orifices or perforations, respectively. Ingard and Labate[1] experimentally observed vorticity and jet formation at an orifice. While the resistance is found to increase with the particle velocity in the perforations, the reactance decreases. The decrease in reactance is associated with a loss of inertial end correction.[2] Various empirical models exist that describe the change of impedance due to high sound pressure levels at single tone actuation, e.g., Refs. 3 and 4. The interaction of multiple high amplitude stimuli is of substantial interest in the design of Helmholtz resonator liners. Bodén studied the acoustic properties of orifices and perforated sheets under high level multi-tone excitation with a focus on harmonically related frequency combinations, see, for instance, Refs. 5–7. He found that the effect of harmonically related multi-tone stimuli on the impedance of orifices is different compared to the excitation with harmonically unrelated stimuli. In a previous work, we experimentally examined the change of impedance of a perforated plate at primary sound field frequencies when an additional secondary high amplitude excitation is used to induce flow separation effects. Thereby, the stimuli were unrelated in terms of frequency and phase. Dependent on the properties of the secondary stimulus, the impedance of the perforated plate at the frequencies of the primary sound field is changed. By means of dimensional analysis, a semi-empirical model for the change of resistance is derived, where the secondary flow is approximated as quasi-steady.[8] The findings bear a certain resemblance to the experiments with orifices under high amplitude excitation and bias flow,[9] as the change of impedance at the primary sound field frequencies results from flow separation induced by the secondary excitation. This study completes the empirical model deduction by accounting for the loss of end correction, caused by the secondary stimulus.

2. Experimental design

The experimental setup as well as the analysis method is described in detail in Ref. 8 and will only be briefly introduced here. Figure 1 depicts the experimental setup. It consists of two identical rectangular duct sections. Each section is equipped with four microphones and one loudspeaker. The perforated plate is clamped between the two sections at $x = 0$. Primary and secondary stimulus are pure tones with frequencies f_p and f_s. The stimuli are unrelated in frequency and phase. Hence, the frequency relation between the stimuli is inharmonic and specific phase relations are disregarded in the measurement process. Consequential, no common relation exists between the measured combinations of primary and secondary excitation. Moreover, only the fundamental frequencies of the stimuli are considered. The study is restricted to the plane wave domain. The primary sound field is varied from 200 to 1600 Hz in steps of 51 Hz. The frequency of the secondary excitation is set to either 331 or 943 Hz. Loudspeaker A, in section 1, is used to excite the primary stimulus with sound pressure $\hat{p}_p$. Loudspeaker B, in section 2, is used to excite the secondary stimulus with sound pressure $\hat{p}_s$. The sound field is decomposed into incident and reflecting components in each section separately.[10] While the secondary

[a)]Also at: German Aerospace Center, Berlin, 10623, Germany.

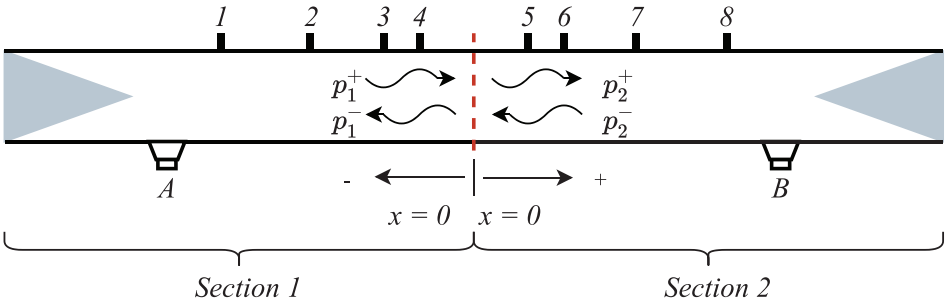

Fig. 1. Schematic description of experimental setup.

sound field is varied in sound pressure level, the primary sound field is kept constant for all f_p at a root mean square (RMS) level of either $\bar{p}^+_{p1,l} = 100$ dB or $\bar{p}^+_{p1,nl} = 135$ dB. The plate impedance is calculated from the plane wave components of the primary sound field at $x = 0$ as

$$\zeta = \frac{\Delta p}{\rho_0 c_0 \hat{u}_p \sigma} = \frac{\hat{p}^+_{p1} + \hat{p}^-_{p1} - \hat{p}^+_{p2} - \hat{p}^-_{p2}}{\hat{p}^+_{p1} - \hat{p}^-_{p1}}. \tag{1}$$

The particle velocities in the perforations due to the primary and secondary sound fields $\hat{u}_p$ and $\hat{u}_s$ are derived from their respective plane wave components at $x = 0$,

$$\hat{u}_p = \frac{\hat{p}^+_{p1} - \hat{p}^-_{p1}}{\rho_0 c_0 \sigma}, \tag{2a}$$

$$\hat{u}_s = \frac{\hat{p}^-_{s2} - \hat{p}^+_{s2}}{\rho_0 c_0 \sigma}. \tag{2b}$$

To depict the results, the amplitudes of the RMS particle velocities $\bar{u}_p$ and $\bar{u}_s$ are used, since they resemble the time averaged absolute particle velocity closely,

$$\frac{\omega}{2\pi}\int_0^{2\pi/\omega} |\hat{u}\sin(\omega t)|dt = \frac{2|\hat{u}|}{\pi} = \frac{2\sqrt{2}|\bar{u}|}{\pi} = 0.90|\bar{u}|. \tag{3}$$

Table 1 depicts the geometric parameters of the plates under study. All specimen considered have a homogeneous hole distribution and the hole geometry is circular with sharp edges. d represents the orifice diameter, h the thickness, and σ the porosity.

3. Results

The effective inertial length L_{in} of an orifice, without flow separation effects present, is given as

$$L_{in} = h + 2\Delta e_{in} \cdot \psi(\sigma), \tag{4}$$

where Δe_{in} is called the inertial end correction accounting for mass moving outside of the orifice. Here, Rayleigh's approximation $\Delta e_{in} = 4d/3\pi$ is used.[11] $\psi(\sigma)$ is a function, accounting for hole interaction effects on the attached mass in perforated plates. For $\psi(\sigma)$, the derivation by Fok is used.[3,12]

We suppose that the effective length, when flow separation is induced by the secondary excitation $L_{in,s}$, can be expressed as

$$L_{in,s} = h + 2\Delta e_{in} \cdot l_s \cdot \psi(\sigma), \tag{5}$$

Table 1. Geometric parameters of the perforated plates.

Sample	σ (%)	d (mm)	h (mm)
P1	1.03	1.5	1
P2	4.09	1.5	1
P3	4.09	2.5	1
P4	6.18	1.5	1

where l_s is a factor accounting for the loss of end correction. l_s can be deduced from the measurements by using dimensionless parameters,

$$\frac{(\mathrm{Im}\{\zeta\} - \mathrm{Im}\{\zeta_p\}) \cdot \sigma}{2\mathrm{He}} = \frac{2\Delta e \cdot \psi(\sigma) \cdot (l_s - 1)}{d}, \tag{6}$$

where $k = \omega/c$ represents the wave number. $\mathrm{Im}\{\zeta\} = k \cdot L_{in,s} \cdot \sigma$ represents the specific mass reactance at f_p of one orifice of the perforated plate, when the secondary excitation is active. $\mathrm{Im}\{\zeta_p\}) = k \cdot L_{in} \cdot \sigma$ represents the specific mass reactance of one orifice without secondary excitation or nonlinear effects due to a high amplitude primary excitation, i.e., the reactance measured for a primary sound field with $\bar{p}^{+}_{p1,l} = 100\,\mathrm{dB}$ and $|\bar{u}_s| = 0$. $\mathrm{He} = \pi f d/c$ is the Helmholtz number. Solving Eq. (6) for l_s we find

$$l_s = \frac{(\mathrm{Im}\{\zeta\} - \mathrm{Im}\{\zeta_p\}) \cdot \sigma \cdot d}{2\mathrm{He} \cdot 2\Delta e \cdot \psi(\sigma)} + 1. \tag{7}$$

Previously, it was demonstrated, that the change of impedance due to a secondary high amplitude excitation, correlates for the inverse Strouhal number $1/\mathrm{St}_{p,d} = |\bar{u}_s|/2\pi f_p d$. For $f_p \ll f_s$, deviating behavior due to unsteady flow conditions of the secondary sound field was observed. The deviations either decrease when the particle displacement of the secondary excitation exceeds the orifice diameter, i.e., $1/\mathrm{St}_{s,d} > 1$, where $1/\mathrm{St}_{s,d} = |\bar{u}_s|/2\pi f_s d$, or with increasing f_p/f_s. For detailed information, see Ref. 8. Results for l_s presented here are restricted to the case $f_p/f_s > 0.75$. Moreover, since a better collapse of data is found for the imposed restrictions, l_s is plotted against the inverse Strouhal number on the basis of h: $1/\mathrm{St}_{p,h} = |\bar{u}_s|/2\pi f_p h$.

Figure 2 depicts the loss factor l_s, for all perforated plates under study, plotted against $1/\mathrm{St}_{p,h}$. As can be seen, l_s is independent of the geometrical parameters d, h, and σ. l_s solely depends on the inverse Strouhal number $1/\mathrm{St}_{p,h}$. For $0.25 \leq 1/\mathrm{St}_p \leq 2$, l_s decreases rapidly until a plateau value of approximately 3/8 is attained, marking the onset of quasi-steady flow conditions, as particle displacement exceeds the orifice dimensions. Hence, the attached mass of the perforated plates at the frequencies of the primary sound field f_p is reduced up to 3/8 of its original value due to the periodic bias flow induced by the secondary excitation. With increasing $1/\mathrm{St}_{p,h}$ the scatter of measurement points increases slightly. The increased scatter could either be due to a change of hole interaction effects with increasing flow separation and/or due to increased measurement inaccuracies at high sound pressure amplitudes.

Furthermore, from Fig. 2 one can deduce that l_s generally follows the form of the function

$$l_s = \kappa + \frac{(1-\kappa)}{1 + 1/St^2_{p,h}}, \tag{8}$$

where κ describes the rate of decay and the plateau value at quasi-steady conditions. To determine κ, Eq. (8) is fitted to the results depicted in Fig. 2 through a direct search optimization method.[13] κ is found to be $\kappa = 0.38$. Inserting κ into Eq. (8) yields an empirical formulation to approximate the loss of end correction of a single orifice at primary sound field frequencies due to flow separation induced by a secondary high amplitude stimulus unrelated in frequency and phase,

$$l_s = 0.38 + \frac{0.62}{1 + 1/\mathrm{St}^2_{p,h}}. \tag{9}$$

Equation (9) can be incorporated in linear impedance models via Eq. (5). The dashed line in Fig. 2 shows Eq. (9) compared to the measurements. Good agreement between the empirical approximation and the measurements is found over the entire measurement range considered. Between $1 \leq 1/\mathrm{St}_{p,h} \leq 2$, l_s is slightly underestimated for P1 (◇ symbols)

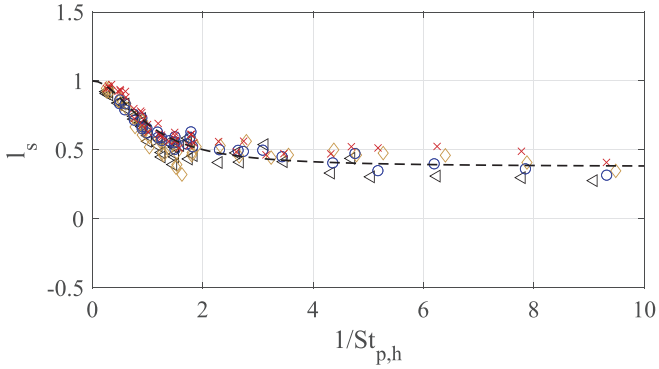

Fig. 2. End correction factor l_s at $\bar{p}^{+}_{p1,l} = 100$ dB for all specimen considered. P1: ◇, $d/h = 1.5$, $\sigma = 1.03\%$ P2: ○, $d/h = 1.5$, $\sigma = 4.09\%$; P3: ×, $d/h = 2.5$, $\sigma = 4.09\%$; P4: ◁, $d/h = 1.5$, $\sigma = 6.18\%$. Dashed line: Eq. (9).

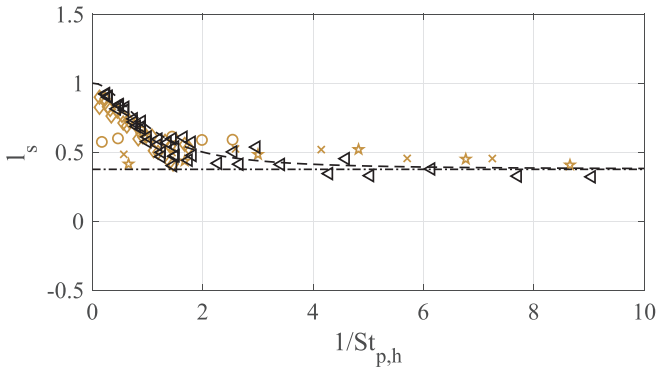

Fig. 3. End correction factor l_s at $\bar{p}^+_{p1,nl} = 135$ dB. P1: ◇; P4: ◁. Dashed line: Eq. (10a). Dash-dotted line: Eq. (10b). Additional symbol reference for P1: f_p [Hz], 255 (⋆), 306 (×), 867 (○); f_s [Hz] 331 (⋆), 331 (×), 331 (○); $1/St_{d,|\bar{u}_s|=0}$, 4.64 (⋆), 3.6 (×), 1.27 (○).

and P4 (◁ symbols). Maximum deviation is found for P1 at $1/\mathrm{St}_{p,h} \approx 1.6$. The result depicts a measurement taken at a limiting case of $f_p = 255$ Hz, $f_s = 331$ Hz, and $|\bar{u}_s| = 2.60$ m/s. Therefore, $f_p/f_s = 0.77$ and $1/\mathrm{St}_{s,d} = 1.08$. Consequential marginal deviations due to unsteady flow conditions of the secondary excitation are expected.

For high amplitude primary sound fields, considerable particle velocities can be induced in the perforations, affecting and mitigating flow separation due to the secondary excitation. Additionally, nonlinear losses of end correction due to the primary sound field are observed without secondary excitation present. Hence, l_s is a function of both sound fields. In case the particle displacement of the primary excitation exceeds the orifice diameter ($1/\mathrm{St}_d > 1$, with $1/\mathrm{St}_d = |\bar{u}_p|/2\pi f_p d$), the flow approximates quasi-steady behavior and the end correction is already significantly reduced without a secondary excitation present. For $1/St_d \leq 1$, the end correction behaves more similar to the case of a linear primary sound field, because the flow separation effects induced by the secondary excitation predominate.[8] Correspondingly, the loss of end correction l_s can be approximated via Eq. (9) for $1/\mathrm{St}_d \leq 1$ and approximates κ in the case $1/\mathrm{St}_d > 1$,

$$l_s = 0.38 + \frac{0.62}{1 + 1/\mathrm{St}^2_{p,h}} \quad \text{if } 1/\mathrm{St}_d \leq 1, \tag{10a}$$

$$l_s = \kappa = 0.38 \quad \text{if } 1/\mathrm{St}_d > 1. \tag{10b}$$

Figure 3 shows Eqs. (10a) and (10b) compared to measurements of l_s for P1 and P4 at a primary sound field with an incident plane wave of $\bar{p}^+_{p1,nl} = 135$ dB. For the low porosity plate P1, comparably high particle velocities arise in the perforations due to the primary excitation. Hence, for low f_p (⋆ and × symbols), the loss of end correction is already at or near its plateau value, indicated by the dash dotted line, representing Eq. (10b). With increasing f_p, l_s approximates the behavior observed for a linear primary sound field. Note that, as $|\bar{u}_p|$ is found to decrease with increasing $|\bar{u}_s|$, no absolute value of $1/St_d$ can be given. For example, for P1 at $f_p = 255$ Hz, we found $1/\mathrm{St}_d = 4.64$ and hence $|\bar{u}_p| = 11.16$ m/s without secondary excitation applied. With increasing $|\bar{u}_s|$ a decrease to $|\bar{u}_p| = 6.80$ m/s at $|\bar{u}_s| = 13.9$ m/s was observed. For the plate P4 with the highest porosity studied, the primary particle velocities induced in the perforations are lower and reduced nonlinear behavior is observed. Accordingly, the end correction behaves more similar to the case of a linear primary sound field with an incident plane wave of $\bar{p}^+_{p1,l} = 100$ dB under high amplitude secondary excitation. Overall, the model yields good agreement to the measured end correction for high pressure primary sound fields.

4. Conclusion

Due to a secondary high amplitude excitation, the impedance of a perforated plate, impacting on a primary sound field, is changed. The present study focuses on experimentally deriving an approximation to estimate the effects of a high amplitude secondary excitation, unrelated in terms of frequency and phase, on the inertial end correction of perforated plates at primary frequencies. The secondary excitation induces flow separation at the edges of the perforations, thereby reducing the inertial end correction of the orifices and consequentially reducing the plates reactance faced by a primary sound field. It is found that the loss of end correction is only dependent on the Strouhal number. Consequential, an empirical expression is derived accounting for the loss of end correction of an orifice, including possible interaction effects of adjacent holes in perforated plates. The model is valid for perforated plates with circular orifices at arbitrary levels of primary and secondary excitation and for ratios of primary to secondary frequencies larger than approximately $f_p/f_s > 0.75$.

Acknowledgments

This study was supported by the project ARTEM (Aircraft noise Reduction Technologies and related Environmental iMpact) which has received funding from the European Union's Horizon 2020 research and innovation programme under Grant No. 769 350.

References and links

[1]U. Ingard and S. Labate, "Acoustic circulation effects and the nonlinear impedance of orifices," J. Acoust. Soc. Am. **22**, 211–218 (1950).
[2]R. Panton and A. Goldman, "Correlation of nonlinear orifice impedance," J. Acoust. Soc. Am. **60**, 1390–1396 (1976).
[3]T. Melling, "The acoustic impedance of perforates at medium and high sound pressure levels," J. Sound Vib. **29**(1), 1–65 (1973).
[4]Z. Laly, N. Atalla, and S. A. Meslioui, "Acoustical modeling of micro-perforated panel at high sound pressure levels using equivalent fluid approach," J. Sound Vib. **427**, 134–158 (2018).
[5]H. Bodèn, "Experimental investigation of harmonic interaction effects for perforates," in *11th AIAA/CEAS Aeroacoustics Conference* (2005), Vol. 2.
[6]H. Bodèn, "Acoustic properties of perforates under high level multi-tone excitation," in *19th AIAA/CEAS Aeroacoustics Conference*, Germany, Berlin (2013).
[7]H. Bodèn, "The effect of high level multi-tone excitation on the acoustic properties of perforates and liner samples," in *18th AIAA/CEAS Aeroacoustics Conference*, Colorado Springs, CO (2012).
[8]R. Burgmayer, F. Bake, and L. Enghardt, "Effects of a secondary high amplitude stimulus on the impedance of perforated plates," J. Acoust. Soc. Am. **149**(5), 3406–3415 (2021).
[9]L. Zhou and H. Bodèn, "The effect of combined high level acoustic excitation and bias flow on the acoustic properties of an in-duct orifice," in *19th AIAA/CEAS Aeroacoustics Conference*, Berlin, Germany (2013).
[10]C. Lahiri, "Acoustic performance of bias flow liners in gas turbine combustors," Ph.D. thesis, Technical University Berlin, Berlin, Germany (2013).
[11]J. W. Strutt and B. Rayleigh, *The Theory of Sound* (Macmillan, New York, 1929), Vol. II.
[12]V. A. Fok, "Theoretical study of the conductance of a circular hole, in a partition across a tube," in *Proceedings of the USSR Academy of Sciences* (1941), Vol. 31, pp. 875–878.
[13]J. C. Lagarias, J. A. Reeds, M. H. Wright, and P. E. Wright, "Convergence properties of the Nelder-Mead simplex method in low dimensions," SIAM J. Optim. **9**, 112–147 (1998).